Proceedings of the 6th ITB International Graduate School Conference

Multidisciplinary Collaboration for Sustainable Energy: Science, Technology, Policy, and Society

Numerical Modeling of the Songa-Wayaua Geothermal Reservoir Incorporating Seawater Intrusion Effects

Permana Jaya Hikmat[1,2], Sutopo[1], & Heru Berian Pratama[1]

[1]Geothermal Engineering Master's Program, Faculty of Mining and Petroleum Engineering, Institut Teknologi Bandung, Jl. Ganesha 10 Bandung 40132, Indonesia
[2]PT PLN (Persero), Jalan Trunojoyo Blok M-1 No.135, Jakarta, Indonesia
Email: permana.jh@gmail.com

Abstract. The Songa-Wayaua Geothermal Working Area (GWA), located in South Halmahera, North Maluku, is a high-enthalpy geothermal system with planned development for 2 × 5 MW power generation. Despite considerable progress in exploration and early-stage modeling, challenges remain in accurately simulating subsurface behavior near the coastline, particularly with regard to seawater intrusion and its impact on reservoir performance. This study presents the development of an updated numerical reservoir model using the Brynhild module within the Volsung geothermal simulation platform. By integrating geological, geophysical, and geochemical data, a refined 3D conceptual model was constructed in Leapfrog and subsequently imported into Brynhild. The model incorporates a multi-component equation of state ($H_2O + CO_2 + NaCl$) to capture the thermodynamic effects of saline intrusion. Boundary conditions and reservoir properties were carefully calibrated to replicate natural state conditions and surface manifestations. Simulation results successfully reproduce pre-exploitation temperature and pressure profiles and demonstrate the extent and direction of seawater intrusion. History matching mass flow and chloride concentrations further validates the model's ability to represent dynamic reservoir behavior. This integrated modeling approach provides critical insights for sustainable geothermal development in coastal settings.

Keywords: *geothermal reservoir, numerical modeling, seawater intrusion, Brynhild, Volsung, Songa-Wayaua, North Maluku.*

1 Introduction

The Songa-Wayaua GWA is situated in the South Halmahera district, North Maluku, covering a total area of approximately 42,540 hectares. This area has been designated for the development of a geothermal power plant with a planned installed capacity of 2 × 5 MW. Preliminary investigations indicate that the reservoir exhibits high-enthalpy characteristics, with subsurface temperatures ranging from 240°C to 250°C—conditions well-suited for efficient geothermal power generation[1].

Despite significant progress in exploration and modeling activities[2][3][4][5], the current numerical reservoir model does not adequately capture the subsurface dynamics, particularly in areas proximal to the coastline. This limitation raises concerns regarding the influence of seawater intrusion on the reservoir's thermodynamic behavior and long-term sustainability.

In response to these challenges, this study aims to develop an updated numerical model of the Songa-Wayaua reservoir using the Volsung simulation software. The modeling effort is coupled with a refinement of the conceptual model, explicitly incorporating the effects of seawater intrusion. This integrated approach is expected to improve the accuracy of the reservoir characterization and support more robust development planning for geothermal exploitation in coastal settings.

2 Geosciences Review

2.1 Geological Review

Previous studies identified [5][6][7][8][10] that the heat source in the Songa-Wayaua geothermal working area originates from magma pockets beneath the intrusions of Mt. Lansa and Mt. Pele. The geothermal reservoir is hosted within faulted metamorphic, old volcanic, and pyroclastic rocks, while the clay caprock is most developed in the Mt. Pele manifestation area, with a thickness of 100–300 meters[11].

From this study, a tentative geological model of the Songa-Wayaua geothermal field was obtainedas in Figure 1. Geothermal prospectivity is structurally controlled by two dominant normal faults. The first trends N140°–145°E and is associated with coastal hot springs and the Bukit Airpanas valley (Wayaua fault). The second trends N25°–45°E and controls surface manifestations in the Mt. Pele area. Mt. Pele is considered the most promising zone due to the dense distribution of alterations and manifestations, whereas Mt. Lansa is interpreted as a young volcanic heat source despite lacking surface manifestations, though hot springs occur at Bakor-bakor hill to its east show at figure 1[11].

Subsurface hot fluids rise beneath Mt. Pele, producing both upflow and outflow features. Upflows emerge as steam vents in Mt. Botak, while outflows form hot springs due to interactions between permeable sedimentary rocks and overlying impermeable Pele lava flows—thinner and more fractured on the eastern slope.

The Pele-Wayaua fault, lying between metamorphic and volcanic units, may serve as a geothermal fluid trap due to its open fault nature and its coverage by low-permeability volcanic rocks. This facilitates accumulation in the permeable Bacan sedimentary unit without surface emergence. Fluids beneath Mt. Lansa, possibly sourced from a separate heat body, migrate eastward and emerge at Bakor-bakor dome due to jointed rocks enabling vertical fluid escape.

Remote sensing further supports the existence of fracture zones in this area, particularly near Bakor-bakor hill. However, no major faults are observed at the surface of Mt. Pele and Mt. Lansa—suggesting that local stratigraphy and minor structural features dominate fluid flow and permeability control.

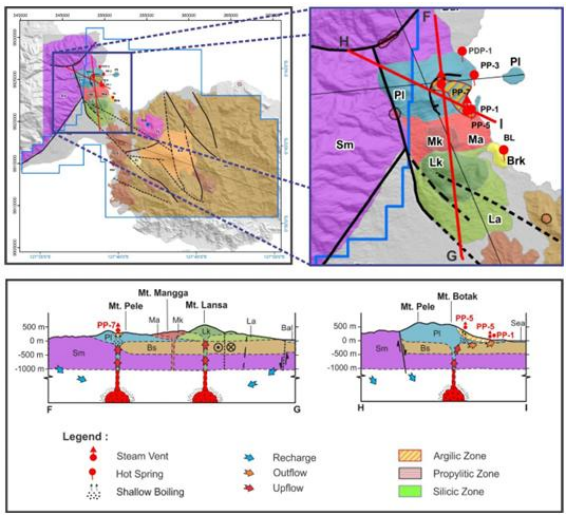

Figure 1 Tentative geological model by PLN and NewQuest. The geological model of geothermal concept in Mt. Pele, the heat source comes from underneath of Bs unit. The permeable zone also composed by Bs unit where the geothermal fluid flows (red arrows) [11].

2.2 Geochemistry Review

Seven hot springs and three fumaroles have been sampled across the Songa-Wayaua geothermal area to characterize the hydrothermal system through chemical and gas geochemical analyses[11]. The hot springs exhibit a range of temperatures from 35°C to 100°C and include boiling springs, mixed hot springs, and coastal springs submerged during high tide.

Boiling spring samples (PP-1 and PP-2) located at the Pele-Pele coastal area, with elevations between 12–17 meters above sea level, record temperatures of approximately 93–100°C. Mixed-type springs, such as PP-3, WAY, PDP-1, PDP-2, and BL, display lower temperatures (35–84°C) and are situated very close to sea level (0–1 masl), suggesting seawater interaction or dilution. Fumarolic activity is evident on the slopes of Mt. Pele, with three steam vents (PP-5 to PP-7) reaching temperatures between 92.9°C and 100.1°C. These were selected for gas geochemical analysis to further understand the deep fluid composition and subsurface processes. Additional samples from cold springs, lake water, and seawater (SONGA, TLG, and SW) were also collected to provide baseline and comparative data for geochemical interpretation. Figure 2 shows the locations of each sample on the field map[11].

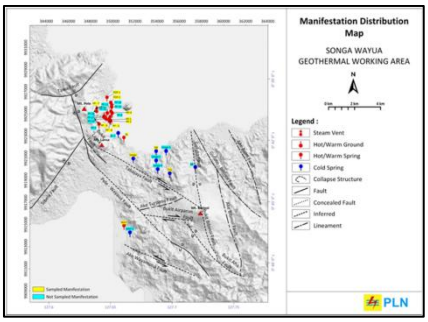

Figure 2 Map of sampled surface manifestation in Songa-Wayaua geothermal working area by PLN and NewQuest [11].

However, the geochemistry review is focused on water geochemistry analysis due to the main goal from this research is to model the seawater intrusion. Liquid sample analysis result from the surface manifestations shows that Pele-Pele and Pado-Pado hot springs dominated by Na-Cl with the concentration of Na around 4,000 – 8,000 ppm and Cl concentration around 7,000 – 14,000 ppm. The pH value of those springs is around 5.6 – 7.5 and have high enough sulfate (SO4), low bicarbonate (HCO3) and high Calcium (Ca). The other hot springs, namely Wayaua hot spring, have sulfate and chloride concentration similar with seawater[11].

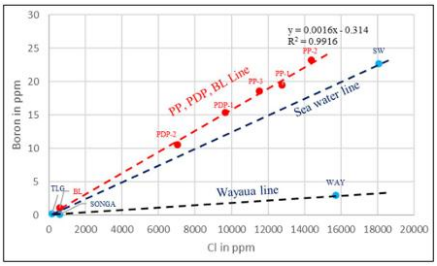

Figure 3 Cl/B ratio of surface manifestation in Songa-Wayaua geothermal working area by PLN and NewQuest [11].

Figure 3 shows that the Cl/B ratio separates the surface manifestations into two different lines. Pele-Pele, Pado-Pado and Bubane Lansa hot springs are situated in one line, while the Wayaua hot spring is plotted in another line. In other words, the Wayaua hot springs have different properties with Pele-Pele and Pado-Pado hot springs [11]. However, both lines look different from the Cl/B ratio of seawater. Figure 4 clearly shows different fluid origins of the existing hot springs. Pele-Pele and Pado-Pado hot springs are in one line, called the geothermal line. Meanwhile, the Wayaua hot springs is situated in the same line as the seawater. It indicates the relationship with seawater through Cl and SO4 content. Seawater intrusion, vertically, is unlikely to occur, since reservoir location difference from geophysical data is between 1000 - 1500 m, with an interference line around 8000 m. However, horizontally, intrusion is likely to occur, because the distance of the reservoir to the seawater interference line is only around 2000-3000 m[11]. The effects of exploitation if not properly maintained can increase the likelihood of seawater intrusion. In addition, it is expected that between the reservoir and the interference line there may be a rock barrier.

Therefore, the data from Wayaua manifestations will be prioritized to be modelled in the reservoir simulation. Other data to be matched is the rate of Pele-Pele manifestations.

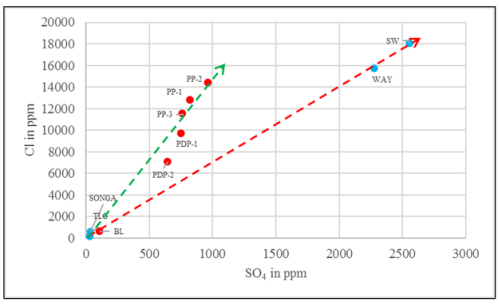

Figure 4 Relationship between Cl and SO4 of surface manifestation in Songa-Wayaua geothermal working area by PLN and NewQuest [11].

Determination of the estimated reservoir temperature is carried out using a variety of standard geothermometers commonly used for liquid and gas. The main goethermometers for determining the temperature are mixing models, T Na-K-Ca, T Na/K and T gases such as D'amore-Panichi, Giggenbach, D'Amore-Truesdell and Arnosson. In estimating the reservoir temperature using liquid and gas geothermometer, it produces good aggrement. Both geothermometer methods provide estimates of Songa's geothermal reservoir temperature around 220 - 240°C.

Geochemical models of geothermal reservoir, as shown in Figure 5, are intended to draw fluid hydrological flow patterns based on temperature lines to determine upflow and outflow areas and integration with geological and geophysical models used to determine target wells in the reservoir. The reservoir geochemical model is made using the NW-SW cross section that passes through Mt. Botak fumarole, Pele-Pele and Bubane Lansa hot springs, in order to fulfill the requirements as a model that contains upflow and outflow areas. Determination of the upflow area generally uses the manifestation of fumarole and is combined with the contours of silica and bicarbonate from the distribution of hot springs. Based on this method it is estimated that the possible upflow area of the geothermal reservoir stretches from the slopes of Mt. Lansa to the slopes of Mt.Pele exceeds Mt Botak fumarole. The temperature of the upflow area based on the count of the geothermometer ranges from 220 – 240°C which is limited by a contour temperature of 220°C. The identified outflow area is in the southwest region limited by the Bubane Lansa hot spring with a temperature line of around 100°C.

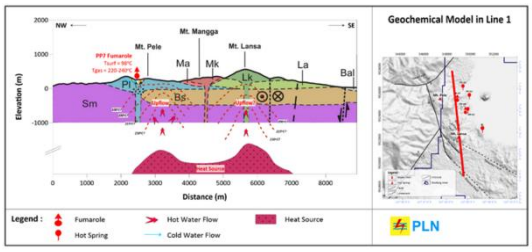

Figure 5 Tentative geochemical model along the geology model cross-section by PLN and NewQuest [11].

2.3 Geophysics Review

Synthesis of gravity, magnetic and MT data generally give a positive result in describing an indication of an area of interest beneath Mt. Pele. Geological and geochemical data give a signature of possible geothermal reservoir occurrence beneath Mt. Pele. MT data gives an indication of an updome-shape resistivity structure beneath Mt. Pele. This indication is also supported by high gravity anomaly as well as an indication of a demagnetized body from magnetic data. However, regarding the RTE anomaly shown in this geophysical integrated analysis (Figure 6), the indication of demagnetized zone that could be associated with prospect area, is represented by a high anomaly. Meanwhile, MEQ events are relatively rare in the prospective area. Some events can be observed beneath Mt. Lansa, while other events are more concentrated at the southern part of Mt. Lansa. The events are likely more correlated with geological structure zone, such as Pele-Wayaua Fault and Bk. Lansa Fault as well as Sibela Fault [11].

An integrated geophysical model, as shown in Figure 7, was then developed in order to summarize the geophysical model derived from gravity, magnetic and MT. The existence of a conductive layer (100 ohm-m) and dense (2.85 gr/cc) body could also be observed at the bottom of the section. Finally, there is a background density of about 2.55 gr/cc and supported by moderate resistivity (10-100 ohm-m). This range of value dominates the distribution of rocks in the Songa-Wayaua geothermal prospect area [11].

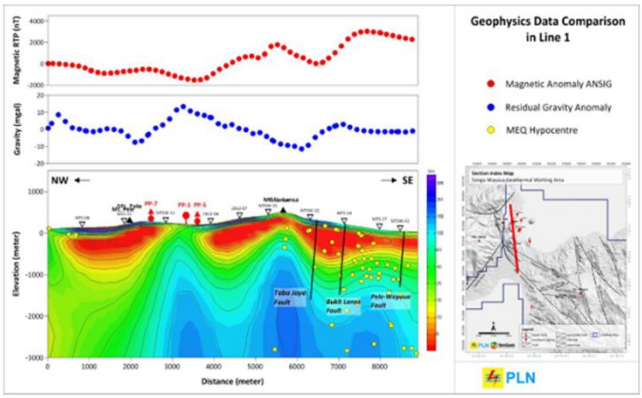

Figure 6 Correlation of Gravity-Magnetic-MT data for identifying Lansa prospect [11].

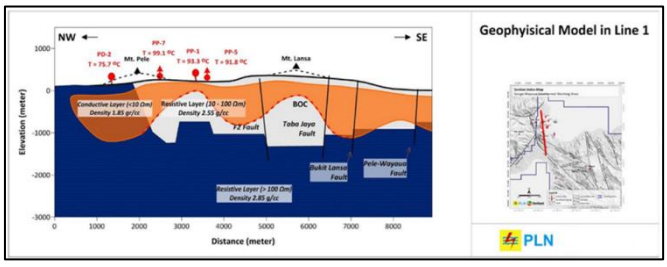

Figure 7 Geophysical model developed by integrating geophysical data in Songa-Wayaua field [11].

2.4 Integrated Conceptual Model

Geologically, the geothermal system of Songa-Wayaua is probably associated with the youngest volcanic product, i.e. Mt. Pele and Mt. Lansa (Figure 8) [15]. The heat source of geothermal system in Songa-Wayaua geothermal prospect is potentially situated beneath Mt. Pele and Mt. Lansa complex. The location probably underneath of Bacan Sedimentary unit (Bs) and Sibela Metamorphic unit (Sm).

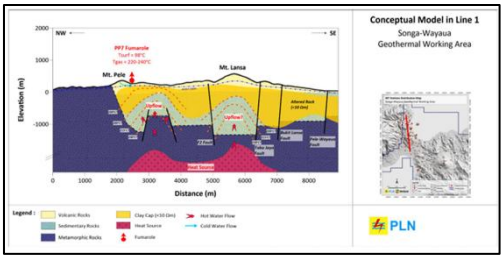

Figure 8 Conceptual model of Songa-Wayaua geothermal system in Line 1 by PLN and NewQuest [11].

Integration of geoscientific data shows that the Songa-Wayaua geothermal system has two indicated upflow zones [11]. The first zone is situated beneath Mt. Pele volcanic complex. The upflow zone is supported by fumarole occurrence (PP-7) discharged on the top of Mt. Pele. The fumarole has higher CO2/H2S ratio and N2/Ar ratio, compared to other fumaroles.

Based on MT data, the upflow zone is characterized by updome-shape resistivity structure as well as thinning of base of conductor layer (Figure 9). Meanwhile, the outflow zone is characterized by thickening of conductive layer toward eastern and southeastern part of Mt. Pele, where the Pele-Pele and Pado-Pado hot springs occur. The trend of CO2/H2S as well as N2/Ar ratio are also lower (PP-8).

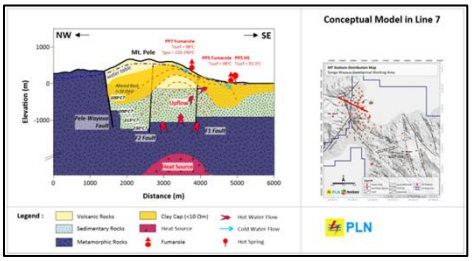

Figure 9 Conceptual model of Songa-Wayaua geothermal system in Line 7 by PLN and NewQuest [11].

The other upflow zone is probably located at Mt. Lansa (Figure 8) [11]. Unfortunately, there is no impressive manifestation on the top of Mt. Lansa. However, the indication of an upflow zone is shown by the MT inversion result. Updome-shape resistivity pattern is indicated beneath Mt. Lansa. There is a hot spring located close to Mt. Lansa, i.e. Bubane Lansa. This hot spring is possibly the outflow from geothermal system in Mt. Lansa. Moreover, the outflow of Mt Lansa is possibly towards northeastern part, where manifestations of Pele-Pele and Pado-

Pado exist. Pado Pado hot springs are more dilute than Pele-Pele hot springs. This may indicate that Pele-Pele is located closer to the source than Pado-Pado (Figure 9) [11]. Based on gas chemistry analysis, gases from (PP-7 & PP-8) are situated on the meteoric line according to the saturated water (ASW) point. It means that there is no indication of magmatic gases. The reservoir temperature is probably in the range of 220-240^{o}C. The top of reservoir is estimated at -100 m elevation. The reservoir rock is possibly formed by volcanic sediment. The integration process to develop 3D conceptual model in Leapfrog based on geological, geochemical and geophysical model can be seen in Figure 10. The Leapfrog model then will be used to build a Volsung reservoir model.

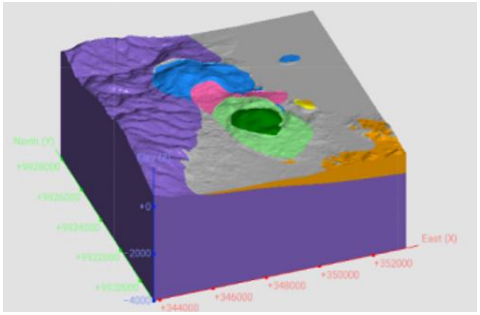

Figure 10 3D Conceptual model from Leapfrog.

3 Reservoir Model

3.1 Model Description

The numerical reservoir model was developed using the Brynhild module within the integrated geothermal modeling platform Volsung. Brynhild supports comprehensive simulation of subsurface reservoirs, wells, and simplified surface facilities. Model construction commenced with the import of a static geological model from Leapfrog, which was integrated into Brynhild as a volumetric dataset.

The model domain spans approximately 4.5 km × 9.5 km, with a vertical extent of about 2.7 km. The upper boundary follows the natural surface topography, while the base of the model extends down to –2000 meters below sea level. To better represent the regional geological orientation, the model was rotated 10 degrees counterclockwise.

To accurately capture fluid behavior, particularly related to seawater intrusion, the model was configured with an equation of state (EOS) that accounts for H_2O + CO_2 + NaCl. This multi-component EOS enables simulation of phase behavior and salinity effects critical for coastal or marine-influenced geothermal systems. The spatial configuration and projection of the Brynhild model, based on the Leapfrog static framework, are presented in Figure 11.

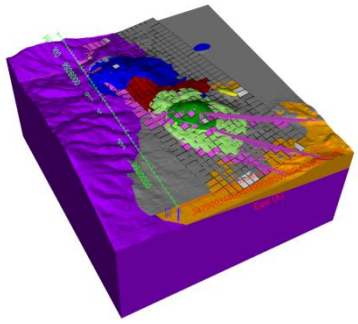

Figure 11 Transferred static model from Leapfrog to Brynhild (Volsung).

3.2 Boundary Conditions

The model employs both Dirichlet and Neumann boundary conditions to represent physical constraints and driving processes within the geothermal system. Dirichlet boundary conditions are applied to the upper and lateral boundaries. At the upper boundary, atmospheric conditions are imposed, with a fixed pressure of 1 bar and an assumed air temperature of 15°C[10]. Lateral boundaries are configured to represent seawater intrusion, approximated by a static seawater column extending from the highest elevation. The corresponding pressure is calculated based on the density of saline water, accounting for the presence of dissolved salts.

Neumann boundary conditions are utilized to simulate dynamic processes. A heat and mass inflow is imposed at the base of the reservoir to represent the upflow of geothermal fluids. Additionally, near-surface boundary conditions are applied to replicate natural discharge features, aiding in achieving a realistic match to the observed natural state of the system. The atmosphere condition blocks, and sea modelled can be seen in Figure 12.

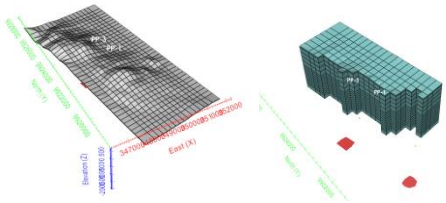

Figure 12 The atmosphere condition blocks, and sea modelled.

3.3 Rock Properties

The transition from the static geological model in Leapfrog to the dynamic reservoir model in Brynhild offers significant advantages in assigning rock and reservoir properties. Brynhild automatically imports the selected volumes, layers, and faults from the Leapfrog model, enabling seamless integration of the geological framework into the simulation environment.

One of the key benefits of this workflow is the ability to assign rock properties directly to geological units based on the imported static model. However, some

limitations arise from the interpolation algorithms used during conversion. In certain cases, inconsistencies may occur, such as simulation blocks not aligning precisely with the original volume definitions. Additionally, when using layer-based top grid types, there may be instances where specific properties are not assigned correctly or entirely omitted from the model.

Brynhild addresses these challenges by providing a comprehensive lithology table interface (shown in Figure 13), which allows users to simultaneously review and edit rock properties across all units. This interface supports efficient calibration and quality control during model setup. Several representative rock types and their associated properties have been incorporated into the model to capture the heterogeneity of the reservoir.

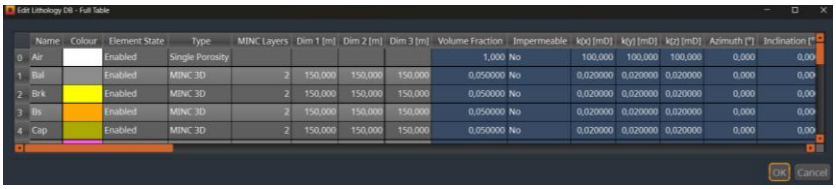

Figure 13 Full lithology table in Brynhild.

3.4 Modeling Results

The primary objective of this numerical simulation was to replicate the pre-exploitation temperature and pressure distributions within the reservoir and to evaluate the potential impact of seawater intrusion on the system. To achieve this, the model was run under steady-state conditions, with the simulation time extending to durations consistent with geological timescales, thereby allowing the system to reach thermodynamic equilibrium.

The simulation outputs were systematically analyzed and compared against available geological, geochemical, and geophysical data [11], as well as field observations—particularly in terms of mass manifestation rates. This comparison provided a means of validating the model and assessing its reliability in representing the natural state of the geothermal system.

The results of the natural state simulation are illustrated in Figure 14, highlighting the model's capability to reproduce key thermal and hydraulic characteristics observed in the field.

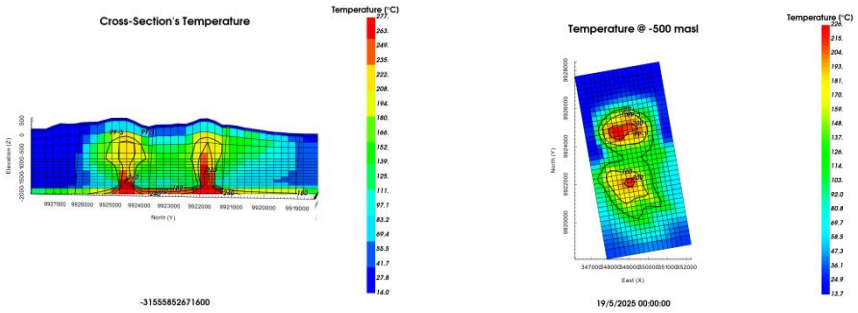

Figure 14 Cross-sectional temperature (left) and elevation sliced (right) result from Natural State simulation run in Brynhild.

Following the successful calibration of the natural state model, the simulation was extended to perform a production history match, with the aim of reproducing observed flow rates and fluid compositions. In Brynhild, this process involves configuring surface springs to represent thermal manifestations, as illustrated in Figure 15 and Figure 16. Measured mass flow rates and chloride concentrations from these surface discharges were used as key calibration targets in the history matching process. To achieve alignment between observed and simulated outputs, the productivity index (PI) values of the springs were iteratively adjusted.

The model successfully achieved a satisfactory match with the observed manifestation data, confirming its capability to reproduce the dynamic behavior of the reservoir under natural discharge conditions, it can be seen in Figure 17.

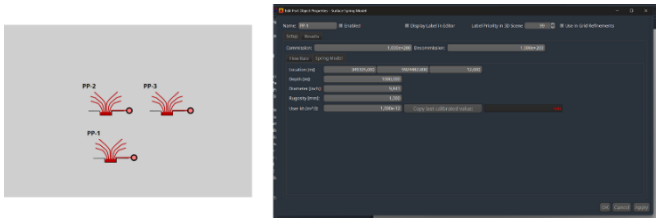

Figure 15 Surface Spring input in Brynhild.

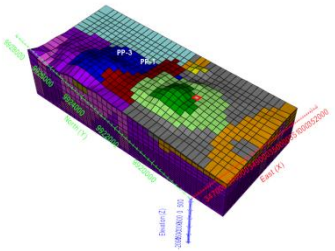

Figure 16 Surface Springs location in 3D view of the reservoir model.

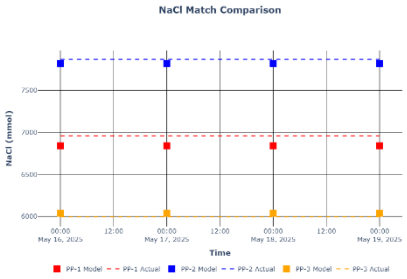

Figure 17 NaCl concentration match comparison between simulation and from data [11].

Figure 18 presents the simulated NaCl concentration distribution, illustrating the influence of seawater intrusion in contributing to fluid inflow into the reservoir. The figure highlights the vertical migration of saline fluid, indicating that seawater penetrates from the uppermost layers down to the deeper sections of the reservoir system.

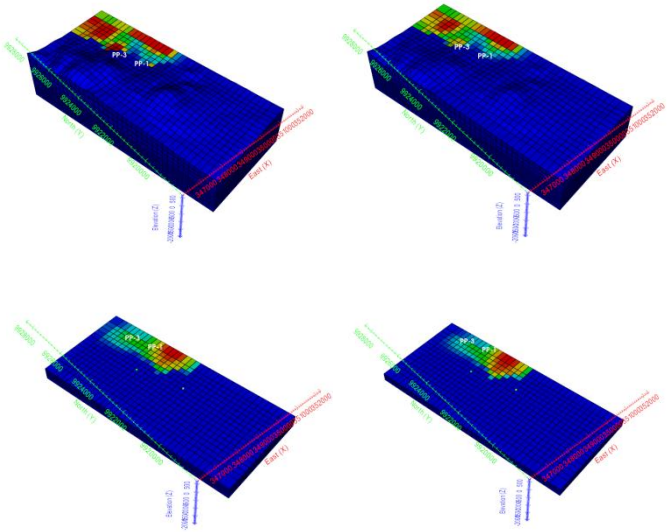

Figure 18 NaCl concentration distribution from top layer to bottom of reservoir layer.

4 Conclusion

This study presents a comprehensive numerical simulation of the Songa-Wayaua geothermal reservoir with explicit consideration of seawater intrusion—a factor critical to understanding subsurface behavior in coastal geothermal systems. Through integration of geological, geochemical, and geophysical data, an updated 3D conceptual model was developed and translated into a dynamic reservoir model using the Volsung-Brynhild platform.

The model effectively simulates pre-exploitation temperature and pressure distributions under steady-state conditions and validates its performance through comparison with field observations and manifestation data. The implementation of a

multi-component EOS ($H_2O + CO_2 + NaCl$) allows the model to capture complex phase behavior and salinity effects, particularly relevant for modeling horizontal seawater intrusion. History matching of surface discharge rates and chloride concentrations further strengthens the model's reliability.

Simulation results indicate that seawater intrudes laterally into the reservoir, influenced by proximity to the coastline and structural permeability. These findings provide valuable insights into the thermodynamic response of the reservoir and highlight the importance of accounting for seawater effects in both model design and long-term resource planning.

5 Future Work Recommendations

Future research on the Songa-Wayaua geothermal reservoir should focus on enhancing model accuracy and applicability through several key advancements. Transitioning from a steady-state to a transient model is crucial for predicting long-term reservoir behavior under various production and reinjection scenarios, particularly to assess the risk of seawater intrusion. Refining coastal boundary conditions with high-resolution offshore geophysical data would improve saline inflow modeling.

Integrating geomechanical analysis would enable evaluation of stress changes and permeability evolution, while geochemical methods such as tracer tests and isotope analysis could validate fluid sources and flow patterns. Additionally, applying inversion techniques and machine learning for model calibration would enhance predictive performance and reduce bias, supporting more effective and sustainable geothermal resource management.

References

[1] ESDM., Potensi Panas Bumi Indonesia Jilid 1 (Jakarta: Direktorat Panas Bumi). 2017.

[2] Kurniawan I, Pratama H B and Adiprana R., A natural state model and resource assessment of Ulumbu Geothermal A natural state model and resource assessment of Ulumbu Geothermal field IOP Conf. Ser.: Earth Environ. Sci. 254. 2019.

[3] Ashat A, Pratama H B and Itoi R., Updating conceptual model of Ciwidey-Patuha geothermal using dynamic numerical model IOP Conf. Ser.: Earth Environ. Sci. 254. 2019.

[4] Manggala Putra R P, Sutopo S and Pratama H B., Improved natural state simulation of Arjuno-Welirang Geothermal field, East Java, Indonesia IOP Conf. Ser.: Earth Environ. Sci. 254. 2019.

[5] Nandiwardhana D., Pemodelan Sistem Panas Bumi Songa – Wayaua berdasarkan Data 3G (Geologi, Geokimia dan Geofisika) Institut Teknologi Bandung. 2017.

[6] Rohmana, Suhandi, Susanto H and Hutamadi R., Penelitian Optimalisasi Pemanfaatan Bahan Galian Daerah Halmahera Selatan, Provinsi Maluku Utara Geological Survey of Indonesia. 2011.

[7] Bakrun, Situmorang T, S B, Sundhoro H, Idral A and H L., Penyelidikan Geolistrik Daerah Panas Bumi Songa-Wayaua, Kabupaten Halmahera Selatan, Maluku Utara Proceeding Pemaparan Hasil-Hasil Kegiat. Lapangan dan Non Lapangan. 2006.

[8] Sumintadireja P., Peningkatan Kualitas / Kuantitas dan Validasi Data Dalam Rangka Penentuan Lokasi Sumur Eksplorasi di Lapangan Songa Wayaua Maluku Utara IOP Conf. Ser.: Earth Environ. Sci. 2012.

[9] Ashat A, Pratama H B and Itoi R., Comparison of resource assessment methods with numerical reservoir model between heat stored and experimental design: Case study Ciwidey Patuha geothermal field IOP Conf. Ser.: Earth Environ. Sci. 254 0–9. 2019.

[10] Hasbi, H.G.F., Hamdani, M.R., Prasetyo, A.G.T., W, A.R.K., Lampuasa,M.J., Sutopo, Pratama, H.B., Prabata, T.W., Application of Numerical Simulation to Update Conceptual Model and Resource Assessment of Songa-Wayaua Geothermal Field. IOP Conf. Series: Earth and Environmental Science 417. 2020.

[11] PLN and NewQuest, Consultancy Services for Pre-Feasibility Study of Songa-Wayaua Geothermal Working Area Financed by Pln Budget Final Report (unpublised). 2020